

Geochemistry of Barail sandstone in Champhai, Mizoram: Implications on provenance and weathering history

Malsawmtluangkima Hauhnar*, Jimmy Lalnunmawia and Orizen M S Dawngliana

Department of Geology, Mizoram University, Tanhril 796 004, India. *Corresponding author. e-mail: mstluangkima@gmail.com

MS received 13 March 2020; revised 22 September 2020; accepted 29 September 2020

Mizoram is geologically young comprising entirely of sedimentary rocks. The Oligocene age of Barail group of sedimentary rocks, exposed near the Indo Myanmar mobile belt, i.e., Champhai area, Mizoram have been studied to infer the provenance and paleoweathering history. The significance of the work is that it will uncover and reconstruct origin of Barail sandstone and restore the tectonic and paleoclimatic conditions based on petrography and geochemistry of the sandstone. The geochemical classification based on diagrams of log(SiO₂/Al₂O₃) vs. log(Na₂O/K₂O) and log(SiO₂/Al₂O₃) vs. log(Fe₂O₃/K₂O) of the Barail sandstones indicated that the sandstones belong to litharenite and wacke. The geochemical characteristics of the rock are plotted in various binary and ternary diagrams and selected ratios of elements are interpreted in the light of source rock characteristics. The Chondrite normalised REE pattern show similar pattern to UCC (Taylor and McLennan 1985) with an enrichment of LREE and depletion of HREE. The ratio of Al₂O₃/TiO₂ and the ternary diagram of La-Th-Sc indicate felsic to intermediate source. Similarly, the high LREE/HREE ratios and negative Eu anomaly (La/Lu)_{cn}, ratios of Eu/Eu*, La/Sc, La/Co, Cr/Th, Th/Sc, Th/Co and Cr/V ratio indicate felsic source. The binary diagram between ratios of Zr/Sc vs. Th/Sc inferred volcanic source. The sediments are also found to be derived from recycled sedimentary rock which is proved by ratios of Zr/Sc and Th/U. The A-CN-K diagram and weathering indices such as CIA, PIA shows moderate to intense weathering in the source area. The investigated Barail sandstones are chemically mature as indicated by the ICV while the ratio of SiO₂/Al₂O₃ indicated moderate sediment maturity.

Keywords. Barail sandstone; Champhai; geochemistry; provenance; weathering.

1. Introduction

The geochemistry of sedimentary rock provide significant role in determining source rock characteristics as indicated by earlier workers (Bhatia 1983; Roser and Korsch 1988; Hayashi et al. 1997; Cullers 2000; Armstrong-Altrin et al. 2004; Rahman and Suzuki 2007; Bhuiyan et al. 2011; Hofer et al. 2012). Due to the immobile nature of

elements during sedimentary process, geochemistry gives more precise information on the study of provenance, tectonic and paleoweathering than petrographic study (Bhatia 1983; Al-Juboury 2007). Further, the elemental ratio of REEs and trace elements also helps in determination of source rock in particular (Taylor and McLennan 1985; Cullers et al. 1988; Cullers 1994, 2000; Cullers and Podkovyrov 2000).

Published online: 05 February 2021

Recently, various workers widely utilised geochemical characteristics of sedimentary rocks to reconstruct provenance, tectonic settings and paleoweathering history in different parts of the world (Armstrong-Altrin et al. 2013; Madhavaraju 2015; Pandey and Parcha 2017; Chaudhuri et al. 2020; Madhavaraju et al. 2016a, b, c, 2017, 2019). A thick sedimentary strata covers the whole region of Mizoram ranging in age from Oligocene to Recent Alluvium. The region is evolved by tectonic upliftment of the Indo-Myanmar collision. The detailed history on the geology, structure and tectonics of the entire region of Tripura-Mizoram-Assam fold belt is well documented by various workers (La Touche 1891; Evans 1964; Karunakaran 1974; Ganguly 1975; Ganju 1975; Behra et al. 2011; Nandy 2017).

The tectono-provenance studies of Surma and Tipam sandstones in Mizoram are carried out by different geologist in few areas of Aizawl and Kolasib. Most of the studies indicated that the sandstones varied from arkose, sublitharenite, litharenite and wacke, and suggested quartzose recycled orogen province and an active continental margin to passive margin setting. The geochemical study also suggested moderate to high intensity of weathering of the provenance (Lalmuankimi et al. 2011; Lalnunmawia et al. 2014, 2016; Lalduhawma and Kumar 2014; Zoramthara et al. 2015; Bharali et al. 2017; Hauhnar et al. 2018; Hussain and Bharali 2019). In other parts of north-east India such as Assam, Manipur and Nagaland, studies on Barail sandstones are well documented by different workers (Srivastava and Pandey 2011; Sen et al. 2012; Rammamoorthy et al. 2015; Kichu and Srivastava 2018). However, the detail insight into the petrological and geochemical study of Barail sandstones in Mizoram is still meagre. Therefore, present work will provide the geochemistry and petrography of Barail sandstone and apply the same in systematic classification of the sandstone, provenance study and determination of intensity of weathering in the provenance.

2. Geological settings

Mizoram is a part of this Neogene Surma Basin comprising a belt of a series of elongated folds that arched in west ward projection. Almost parallel to the suture zone of Arakan–Toma subduction, this Fold belts is elongated in the N–S direction. Stratigraphically, three groups of rock such as

Barail (Oligocene), Surma (Lower to Middle Miocene) and Tipam Group (Upper Miocene to early Pliocene) forms the entire sedimentary succession. Surma Group of rocks comprises of two formation, i.e., Bhuban and Bokabil Formation. Bhuban Formation cover a thickness of about 5000 m and further subdivided into Lower, Middle and Upper Bhuban units. The repetitive successions of arenaceous and argillaceous rocks cover the whole sedimentary formation. The lithology mainly composed of siltstone, shale sandstone, mudstone and various admixture. Few deposits of calcareous sandstone, shell limestone and intraformational conglomerate are also present (Tiwari and Kachhara 2003). The study area of Champhai town is the district capital of Champhai District located in the eastern part of Mizoram adjoining Myanmar to the east and south and Manipur to the north. The area is falling within the geographical coordinates of 23°24′54″-23°26′42″N latitude and $93^{\circ}19'48''-93^{\circ}21'40''$ E longitude (figure 1). lithostratigraphic succession of Mizoram proposed by Karunakaran (1974) and Ganju (1975) indicated that the terrain within Champhai District falls under Barail Group of rock where the mountain ranges are folded into a series of N–E trending anticline and syncline. The geology of the study area mainly comprises of an intercalation of shale, sandstone and siltstone which are gentle to steep slopes with dip ranging from 14° to 45° due west and south-west.

3. Methodology

Twenty five sandstone samples collected from Barail formation, Champhai area were send to Hindusthan Minerals and Natural History specimens Supply Co. Kolkata for thin section preparation. Modal analysis was performed by following Gazzi-Dickinson point counting method (cf. Ingersoll et al. 1984) using Leica DME2700 P petrological microscope equipped with Leica DFC420 camera and Leica Image Analysis software (LAS-v4.6) installed at the Department of Geology, Mizoram University.

Selected 20 sandstone samples were analysed for major/minor oxides, trace elements and REEs using HR-ICPMS and XRF at National Geophysical Research Institute (NGRI). Major oxide concentration was performed using Philips model PW 2440 MagiX PRO wavelength dispersive X-ray Fluorescence spectrometry (WD-XRF) equipped

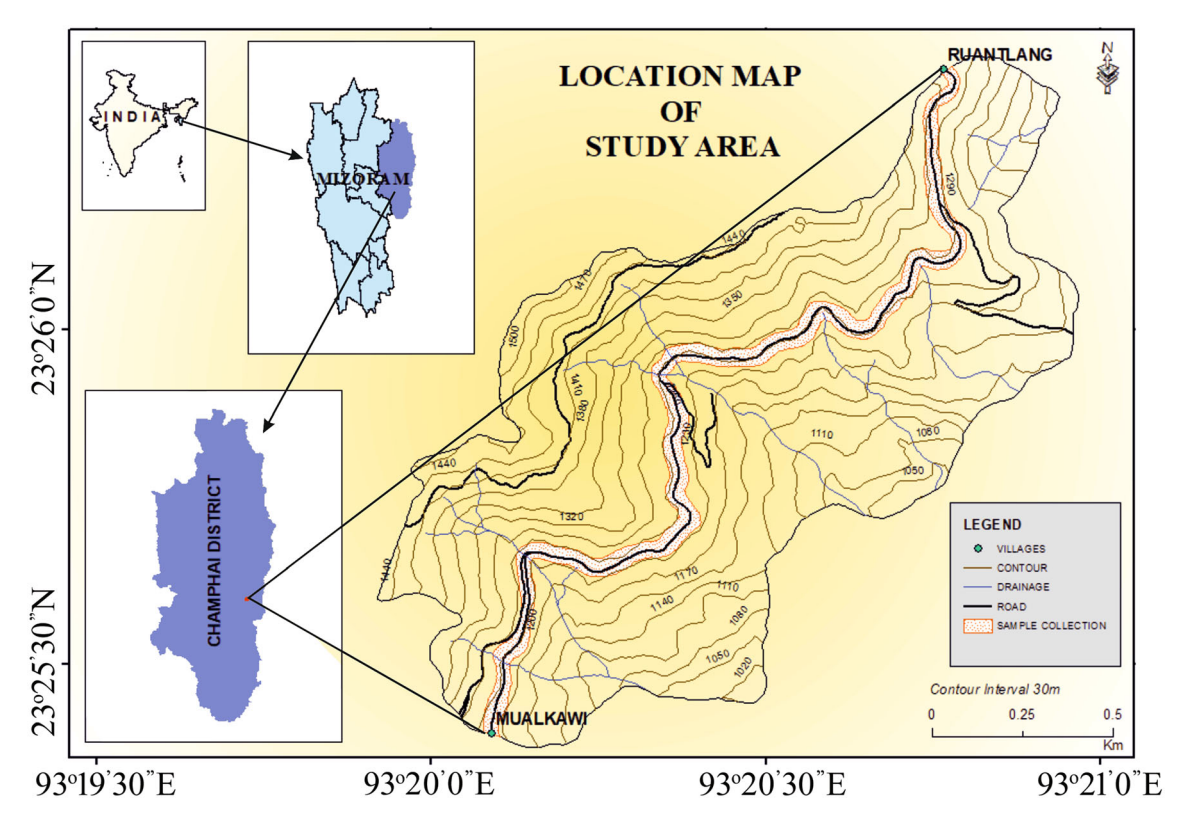


Figure 1. Location of the study area.

with automatic sample changer Model PW 2540 and Software super Q 3.0. The samples were crushed and grinded manually into such fineness as 200 ASTM mesh size. Pressed Pellets were prepared from each of the powdered samples using boric acid in collapsible aluminium cups and then pressed at a pressure of 25 tonnes in two cycles (5 sec each). The Aluminium pellet collapses and the powdered materials stay intact. The samples were then analysed under WD-XRF.

For geochemical analysis of trace element and REE, 0.05 g of grinded powder from each of the samples was weighted and put in a Savillex. To each of the samples, an acid mixture of 7(HF): 3(HNO₃) was added and the Savillex vessels were tightly closed and kept on a hot plate at ~ 150 °C for 48 hrs. After the following 48 hrs, the vessels were open and 1 to 2 drops of HClO₄ was added and evaporated for about one hour to near dryness. The remaining residues were dissolved by adding 10 ml of 1:1 HNO_3 . After all the residues were dissolved, the samples were again kept in a hot plate for 30-40 min at 80°C to dissolve all suspended particles and was transferred into 250 ml standard flask. 10 ml of 1:1 HNO₃ and Rhodium (Rh) solution was added again in the standard flask with Millipore water. Here, Rhodium (Rh) solution

is used as an internal standard. Finally, 5 ml was taken out from 250 ml solution of the samples and was made 50 ml with Millipore water and the final solution was stored in Eppendorf tubes for High Resolution-ICPMS analysis at National Geophysical Institute, Hyderabad. The HR-ICPMS was calibrated with Chinese geochemical standard GSR. To calculate the Loss of Ignition (LOI), each sample with crucibles was subjected to a high temperature flame of 950°C inside a kiln for around 1 hr.

4. Results

4.1 Petrography

Microscopic study of thin section of Barail sandstone revealed that the sandstones were fine to very fine grained, moderately sorted and angular to subangular grains cemented by silica and ferruginous cementing materials. The framework grains of Barail sandstone comprised of Quartz (monocrystalline, Q_m and polycrystalline, Q_p), K-feldspar, plagioclase, and rock fragments with accessory minerals. Modal analysis was performed by following Gazzi-Dickinson (cf. Ingersoll *et al.* 1984) point counting method (tables 1 and 2). Quartz formed the most abundant grains which constitute an average of 72.71% of the total framework grains as shown in table 1. They are angular to sub-angular, rounded to sub-rounded in shape (figure 2b). Among the quartz grains, monocrystalline quartz dominates over polycrystalline quartz and most of the monocrstalline quartz grains are undulatory with wavy extinction. Quartz grains are characterised by concavo convex, overgrowth and suture contact grain boundary.

Feldspar, the least abundance among the framework grain constitutes an average of about 3.87% (table 1). Plagioclase, microcline and orthoclase are observed in thin sections (figure 2c-e). Rock fragments constitute an average of 21.87% of the total grains (table 1) and consist of metamorphic fragments such as gneiss and schist with chert. Mica group of minerals like biotite and muscovite with kink band shape are also observed in the thin sections. The recalculated values of detrital grains are plotted in QFL triangular diagram of Folk (1974) and Dickinson et al. (1983). As a result from the QFL plots (Folk 1974), the barail sandstone samples falls within the fields of litharenite and sublitharenite (figure 3a). The QFL plot of Dickinson et al. (1983), suggests derivation of the investigated sandstone from quartzose recycled orogen (figure 3b).

4.2 Geochemistry

4.2.1 Major oxides

The major element concentrations of the analysed sandstone are given in table 3. The Barail sandsamples mostly stone are rich in SiO_2 (62.45-77.22%) followed by Al_2O_3 (9.69-18.04%), Fe_2O_3 (3.72–10.01%). TiO_2 (0.48–1.23%), MnO (0.04-1.80%), CaO (0.07-0.32%) and P_2O_5 (0.07-0.15%) have a low content as compared to other elements. The SiO₂ abundances increase as ${\rm TiO_2,\ Al_2O_3,\ Fe_2O_3,\ MnO,\ CaO,\ MgO\ and\ K_2O}$ decrease, which suggested a cratonic and recycled sediments associated with passive margin provenances. The Na₂O content increases with increase in SiO₂ content. The high rate of quartz shows the mineralogical maturation (Bhatia 1983). The higher ratio of K_2O/Na_2O (avg. = 1.74%) suggested the enrichment of K feldspar over plagioclase in the studied sandstone.

The log(SiO₂/Al₂O₃) vs. log(Na₂O/K₂O) classification diagram indicated that the Barail

sandstones are classed under greywacke and litharenite (after Pettijohn et al. 1972) (figure 4a). Similarly, the $\log(\mathrm{SiO_2/Al_2O_3})$ vs. $\log(\mathrm{Fe_2O_3/K_2O})$ classification diagram indicated that majority of the samples are classed under wacke and litharenite, though a few clustered under shale and Feshale/sandstone (after Herron 1988) as shown in figure 4(b).

The trace elements of the investigated sandstones are tabulated in table 4. The LIL elements like Ba (avg. = 337 ppm), Sr (58 ppm) and Rb (67 ppm) are lower than UCC (Taylor and McLennan 1985), while HFS elements like Th (avg. = 17 ppm), Y (27) and Zr (448 ppm) arehigher than the standard. The concentration of Zr (avg. = 448 ppm) is exceptionally higher in the analysed samples as compared to UCC. The Barail sandstones are characterised by high concentration of transition elements (Zn = avg. 202ppm; Cu = 98 ppm; Ni = 41 ppm; Cr = 122 ppm and V = 88 ppm) in comparison with the UCC values. The bi-variant correlation of Al₂O₃ against trace elements is given in figure 5. Rb (avg. = 0.59), Sr (avg. = 0.51) and V (avg. = 0.78) exhibit a moderate positive correlation, while few trace elements like Th (avg. = 0.04 and Nb (avg. = 0.20) showed weak positive correlation with Al_2O_3 . Among those elements, Zr (R = -0.11) showed negative correlation with Al₂O₃ which is due to the relatively higher concentration of zirconium in one sample. The positive correlation of Rb with K_2O (R = 0.95) implies that the elements controlled by clay minerals and concentrated during weathering (Ramachandran et al. 2015; Pandey and Parcha 2017).

4.2.2 Rare earth elements

The REEs concentrations of the investigated sandstones are tabulated in table 5. The total REE (\sum REE) concentration ranges between 90.55 and 342.52 ppm with an average of 182.13 ppm which is higher than UCC (Taylor and McLennan 1985). The ratio of \sum LREE/ \sum HREE is between 6.95 and 13.61 ppm with an average of 10.03 ppm which is higher than UCC. The chondrite normalised REEs of Barail sandstones after Taylor and McLennan (1985) indicated the enrichment of light rare earth elements (LREE La–Sm) with negative Eu anomaly (Eu/Eu* = 0.71) (figure 6). The pattern of REE enrichment and depletion of sandstone resemble the pattern of UCC. The Eu/Eu*

Table 1. Modal count of petrographic study of thin section of Barail sandstone.

			Qua	ırtz								
Sample	Monoci	ystalline	quartz	Polycry	ystalline	quartz	$ \text{Total} \\ \text{Q} = $	Fel	dspar	$\begin{array}{c} { m Total} \\ { m F}= \end{array}$	Rock fragment/lithic	
no.	Q_{mu}	Q_{mnu}	Q_{mt}	Q_{p2-3}	$Q_{p>3}$	Q_{pt}	$Q_{\rm mt}$ $+Q_{\rm pt}$	F_{k}	$P_{\rm ca/Na}$	$(F_k+P_{ca/Na})$	fragment	Chert
RM2	56.23	18.27	74.50	2.07	5.18	7.25	81.75	3.00	2.00	5.00	12.75	0.50
RM4	60.95	8.05	69.00	4.44	5.56	10.00	79.00	2.25	1.50	3.75	14.75	2.50
RM5	62.94	5.31	68.25	2.11	5.14	7.25	75.50	3.50	2.75	6.25	16.00	2.25
RM7	41.48	17.77	59.25	1.75	7.50	9.25	68.50	4.00	1.00	5.00	23.75	2.75
RM11	57.93	6.57	64.50	1.90	7.60	9.50	74.00	2.00	0.50	2.50	21.75	1.75
RM12	50.96	11.54	62.50	2.23	5.02	7.25	69.75	2.25	1.50	3.75	24.25	2.25
RM14	56.88	15.12	72.00	0.90	3.60	4.50	76.50	2.75	1.25	4.00	18.50	1.00
RM15	49.79	12.96	62.75	1.92	3.83	5.75	68.50	2.50	1.25	3.75	25.75	2.00
RM16	58.11	6.39	64.50	2.56	3.69	6.25	70.75	2.25	1.75	4.00	23.50	1.75
RM17	59.60	12.15	71.75	1.00	5.50	6.50	78.25	1.75	1.25	3.00	17.25	1.50
RM18	58.44	7.31	65.75	1.27	4.23	5.50	71.25	1.75	0.75	2.50	25.00	1.25
RM19	59.41	11.09	70.50	2.18	5.07	7.25	77.75	2.25	2.00	4.25	15.00	3.00
RM23	59.92	11.08	71.00	0.67	1.33	2.00	73.00	1.00	0.75	1.75	24.50	0.75
RM26	58.68	7.07	65.75	1.50	2.75	4.25	70.00	2.50	1.50	4.00	24.25	1.75
RM27	62.99	5.01	68.00	0.87	1.38	2.25	70.25	2.50	1.75	4.25	23.00	2.50
RM30	56.96	13.54	70.50	1.89	3.61	5.50	76.00	2.75	2.00	4.75	17.00	2.25
RM31	54.96	9.29	64.25	2.07	4.43	6.50	70.75	3.25	2.75	6.00	20.75	2.50
RM33	55.00	11.00	66.00	0.69	1.56	2.25	68.25	1.00	0.75	1.75	28.25	1.50
RM34	53.32	12.93	66.25	1.65	3.85	5.50	71.75	2.50	0.75	3.25	21.00	2.25
RM35	46.00	15.75	61.75	2.00	4.00	6.00	67.75	2.50	1.50	4.00	26.25	2.00
RM36	62.74	8.26	71.00	1.50	4.50	6.00	77.00	1.50	0.75	2.25	19.50	1.25
RM39	51.39	10.86	62.25	2.67	5.33	8.00	70.25	3.00	2.00	5.00	22.25	2.50
RM40	53.12	8.63	61.75	1.50	4.50	6.00	67.75	2.50	1.75	4.25	24.00	4.00
RM41	53.59	7.66	61.25	2.73	7.52	10.25	71.50	1.75	1.25	3.00	23.50	2.00
RM45	53.15	11.10	64.25	2.01	5.74	7.75	72.00	1.50	1.25	2.75	22.50	2.75
Average	55.78	10.59	66.37	1.84	4.50	6.34	72.71	2.34	1.45	3.79	21.40	2.02

Table 2. Key to counted petrographic classes and recalculated parameters.

Petrographic classes		
Quartz	Q_{mu}	Monocrystalline undulatory quartz
	Q_{mnu}	Monocrystalline nonundulatory quartz
	Q_{mt}	Total monocrystalline quartz
	Q_{p2-3}	Polycrystalline quartz with 2–3 grains per quartz
	$Q_{p>3}$	Polycrystalline quartz with $Q_p > 3$
	$ m Q_{pt}$	Total polycrystalline quartz
	Q	Total no. of quartz
Feldspar	F_k	K-feldspar
	$P_{\rm ca/Na}$	Plagioclase feldspar
Lithic fragments/rock fragments	L/R	Lithic fragments or rock fragments
		(sedimentary, metamorphic and volcanic)
Recalculated parameters	Q	$ m Q_{mt} + m Q_{pt}$
	F	$ m F_k + P_{ca/Na}$

anomaly of the studied sandstone ranges from 0.54 to 0.81 (avg. = 0.71), while Ce/Ce* anomaly ranges from 0.93 to 1.27 (avg. = 1.00). Since the value of Ce/Ce* ratio are approximately showing 1, it

exhibits no anomaly (Oni et al. 2014). However, the negative Eu* anomaly and light Ce* anomalies indicate marine depositional environment (Pandey and Parcha 2017).

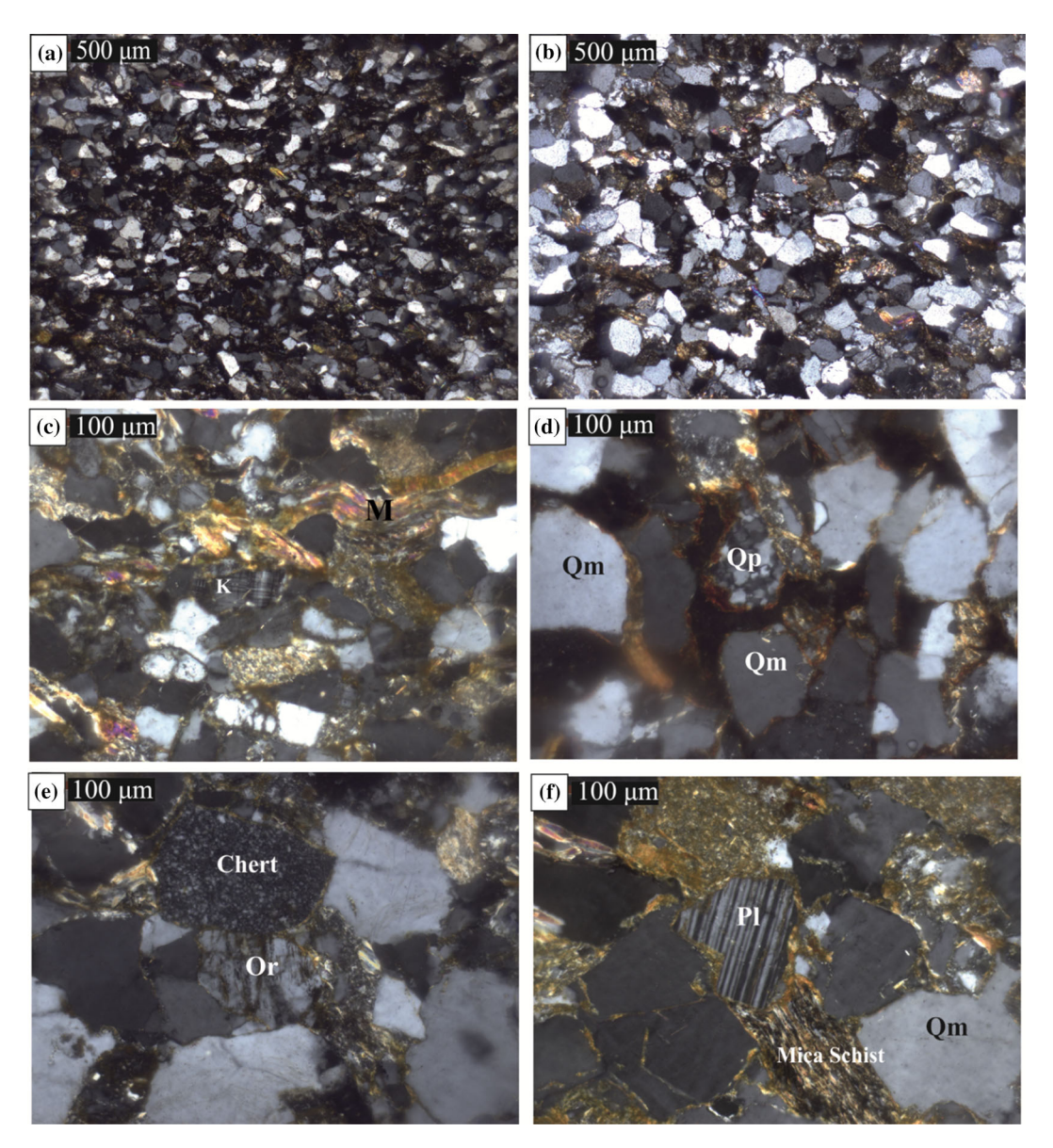


Figure 2. Photomicrograph of Barail sandstones showing $(\mathbf{a}-\mathbf{b})$ fine to very fined grained, angular to sub-angular grains, $(\mathbf{c}-\mathbf{f})$ framework grains such as monocrystalline quartz (Q_m) , polycrystalline quartz (Q_p) , plagioclase (Pl), K-feldspar (M), orthoclase (Or), muscovite (M) and lithic fragments (chertz, Mica schist).

5. Discussions

5.1 Provenance

The provenance of clastic sediments has been established through geochemical studies by various workers (Cullers 1995; Amstrong-Altrin et al. 2004, 2013; Pandey and Parcha 2017). Major oxide data are plotted using discriminant function diagram proposed by Roser and Korsch (1988) to determine the provenance (figure 7a). The diagram indicated that most of the samples clustered within quartzose sedimentary provenance field, though few samples fall within intermediate igneous field

and mafic igneous field. The discriminant function diagram shows that the Barail sandstone is derived from recycled mature continental provenance. The abundance of geochemical concentration and ratio of elements reveal the nature of their source rock. The ${\rm Al_2O_3/TiO_2}$ ratio has been used to infer the source rock of the sediments (Hayashi et al. 1997; Madhavaraju et al. 2016a, b, c) classified into different types of source rocks depending on the abundance of ${\rm Al_2O_3/TiO_2}$ ratio. The ${\rm Al_2O_3/TiO_2}$ ratio ranging between 3 and 8 are represented as mafic, while the ratio ranging from 8 to 21 indicate intermediate and 21–70 as felsic source rock. Since the Barail sandstone exhibit ${\rm Al_2O_3/TiO_2}$ ratio

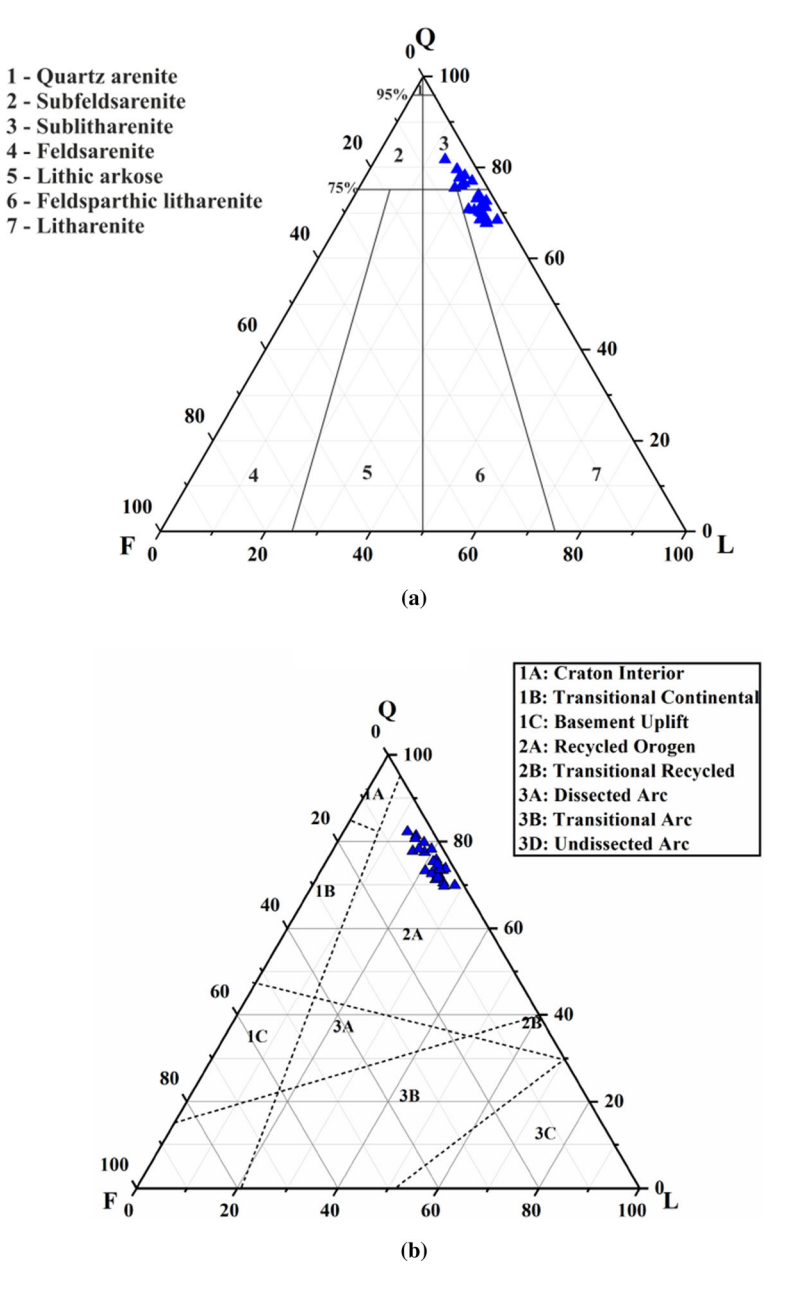


Figure 3. QFL plot of Barail sandstones in Champhai for (a) classification after Folk (1974) and (b) tectonic settings after Dickinson *et al.* (1983).

ranging from 9.7 to 22.21 with an average of 16.83, it is suggested that they are derived from intermediate source rock.

The signatures of source rock can be determined by the nature of REE pattern and size of Eu anomaly in sedimentary rocks (Taylor and McLennan 1985; Armstrong-Altrin et al. 2013; Madhavaraju et al. 2016a, b, c). In general, the felsic source indicates the high LREE/HREE ratios and negative Eu anomaly, while the low LREE/HREE ratios and absence of Eu anomaly characterised mafic source rock (Cullers 1994). Thus the Barail sandstone exhibits high

LREE/HREE ratios (avg. = 10.03) and negative Eu anomaly (avg. = 0.71) which suggest felsic igneous source derivation.

The ratio of elements such as $(\text{La/Lu})_{\text{cn}}$ (8.21–21.63), Eu/Eu^* (0.54–0.81), La/Sc (2.21–7.14), La/Co (0.86–7.50), Cr/Th (3.39–15.42), Th/Sc (1.01–3.43), and Th/Co (0.27–3.60) determined the provenance of sedimentary rocks (Cullers *et al.* 1988; Cullers 1994, 2000; Cullers and Podkovyrov 2000; Armstrong-Altrin *et al.* 2013). In comparison with the presumed ranges of elemental ratio in sediments from felsic, mafic source rock and upper continental

Table 3. Major/minor element concentration (wt.%) of Barail sandstones in Champhai.

Sample	SiO_2	Al_2O_3	${ m TiO_2}$	$\mathrm{Fe_2O_3}$	MgO	MnO	CaO	Na_2O	K_2O
CM1	75.42	10.48	0.63	4.63	1.17	0.31	0.20	1.22	1.55
CM3	69.56	14.36	0.91	5.30	1.65	0.04	0.25	1.01	2.44
CM4	76.76	10.57	0.52	4.23	1.00	0.05	0.07	0.90	1.37
CM7	67.51	12.03	0.70	8.74	1.39	0.08	0.14	1.31	1.54
CM8	75.42	11.45	0.63	3.94	1.14	0.03	0.16	1.19	1.64
CM10	67.01	14.73	0.82	5.94	1.95	0.04	0.27	1.39	2.30
CM12	77.20	10.24	0.50	4.00	1.16	0.08	0.09	1.18	1.48
CM14	63.73	18.04	1.02	5.31	1.38	0.05	0.11	1.00	2.58
CM16	71.14	12.08	0.67	6.09	1.40	0.39	0.15	1.08	1.59
CM18	76.95	9.69	0.86	5.11	1.06	0.09	0.19	1.21	1.52
CM23	76.75	9.96	0.48	4.59	1.16	0.14	0.16	1.15	1.53
CM24	74.61	11.74	0.58	4.12	1.27	0.08	0.21	1.22	1.85
CM26	74.94	11.04	0.69	3.87	1.04	0.03	0.19	1.21	1.92
CM31	66.22	13.99	0.63	6.57	1.11	1.80	0.19	2.15	1.18
CM33	62.45	15.77	1.23	10.01	1.31	0.06	0.04	0.40	1.71
CM34	68.05	15.11	1.01	5.22	1.28	0.11	0.32	1.30	1.89
CM36	73.56	10.89	0.89	4.74	1.21	0.18	0.22	1.11	1.58
CM39	77.22	10.31	0.50	3.72	1.23	0.02	0.13	1.23	1.74
CM41	75.59	9.96	1.03	4.79	1.18	0.03	0.23	1.08	1.15
CM45	75.89	10.93	0.80	4.91	1.26	0.03	0.14	1.14	1.94
UCC	66.00	15.20	0.50	5.00	2.20	0.08	4.20	3.90	3.40
Sample	P_2O_5	LOI	$\mathrm{SiO}_{2}/\mathrm{Al}_{2}\mathrm{O}_{3}$	$\mathrm{Fe_2O_3}/$	$ m K_2O$	${ m Na_2O/K_2O}$	CIA	PIA	ICV
CM1	0.09	3.27	7.20	2.9	9	0.79	72.14	78.78	0.93
CM1 CM3	$0.09 \\ 0.10$	$3.27 \\ 2.96$	7.20 4.84	$\frac{2.99}{2.1}$		$0.79 \\ 0.41$	72.14 75.12	78.78 84.71	
					7				0.81
CM3	0.10	2.96	4.84	2.1	7 9	0.41	75.12	84.71	$0.81 \\ 0.77$
CM3 CM4	$0.10 \\ 0.09$	$2.96 \\ 3.05$	4.84 7.26	$\frac{2.1}{3.09}$	7 9 8	$0.41 \\ 0.66$	75.12 77.38	84.71 84.97	0.81 0.77 1.16
CM3 CM4 CM7	0.10 0.09 0.10	2.96 3.05 5.20	4.84 7.26 5.61	2.1 3.09 5.66	7 9 8 0	0.41 0.66 0.85	75.12 77.38 74.69	84.71 84.97 81.14	0.81 0.77 1.16 0.76
CM3 CM4 CM7 CM8	0.10 0.09 0.10 0.10 0.12	2.96 3.05 5.20 2.62 3.52	4.84 7.26 5.61 6.59 4.55	2.1° 3.09 5.66 2.40	7 9 8 0 8	0.41 0.66 0.85 0.73 0.60	75.12 77.38 74.69 74.00 73.66	84.71 84.97 81.14 81.14 81.51	0.81 0.77 1.16 0.76 0.86
CM3 CM4 CM7 CM8 CM10 CM12	0.10 0.09 0.10 0.10	2.96 3.05 5.20 2.62 3.52 2.58	4.84 7.26 5.61 6.59 4.55 7.54	2.1° 3.09 5.66 2.40 2.5	7 9 8 0 8	0.41 0.66 0.85 0.73	75.12 77.38 74.69 74.00	84.71 84.97 81.14 81.14	0.81 0.77 1.16 0.76 0.86 0.83
CM3 CM4 CM7 CM8 CM10 CM12 CM14	0.10 0.09 0.10 0.10 0.12 0.08 0.10	2.96 3.05 5.20 2.62 3.52 2.58 4.86	4.84 7.26 5.61 6.59 4.55 7.54 3.53	2.1' 3.00 5.66 2.44 2.56 2.70 2.00	7 9 8 0 8 0 6	0.41 0.66 0.85 0.73 0.60 0.80 0.39	75.12 77.38 74.69 74.00 73.66 73.42 79.55	84.71 84.97 81.14 81.14 81.51 80.41 89.21	0.81 0.77 1.16 0.76 0.86 0.83
CM3 CM4 CM7 CM8 CM10 CM12 CM14	0.10 0.09 0.10 0.10 0.12 0.08 0.10	2.96 3.05 5.20 2.62 3.52 2.58 4.86 4.30	4.84 7.26 5.61 6.59 4.55 7.54 3.53 5.89	2.1' 3.00 5.60 2.44 2.55 2.70 2.00 3.80	7 9 8 0 8 0 6 3	0.41 0.66 0.85 0.73 0.60 0.80 0.39 0.68	75.12 77.38 74.69 74.00 73.66 73.42 79.55 76.21	84.71 84.97 81.14 81.14 81.51 80.41 89.21 83.48	0.81 0.77 1.16 0.76 0.86 0.83 0.63
CM3 CM4 CM7 CM8 CM10 CM12 CM14 CM16 CM18	0.10 0.09 0.10 0.10 0.12 0.08 0.10 0.10	2.96 3.05 5.20 2.62 3.52 2.58 4.86 4.30 3.71	4.84 7.26 5.61 6.59 4.55 7.54 3.53 5.89 7.94	2.1' 3.00 5.6i 2.4' 2.5i 2.7' 2.00 3.8i 3.30	7 9 8 0 8 0 6 3 6	0.41 0.66 0.85 0.73 0.60 0.80 0.39 0.68 0.80	75.12 77.38 74.69 74.00 73.66 73.42 79.55 76.21 70.88	84.71 84.97 81.14 81.14 81.51 80.41 89.21 83.48 77.50	0.81 0.77 1.16 0.76 0.86 0.83 0.63 0.94
CM3 CM4 CM7 CM8 CM10 CM12 CM14 CM16 CM18	0.10 0.09 0.10 0.10 0.12 0.08 0.10 0.10 0.10 0.08	2.96 3.05 5.20 2.62 3.52 2.58 4.86 4.30 3.71 2.87	4.84 7.26 5.61 6.59 4.55 7.54 3.53 5.89 7.94 7.71	2.1' 3.09 5.66 2.44 2.56 2.70 2.00 3.88 3.30	7 9 8 0 8 0 6 3 6 0	0.41 0.66 0.85 0.73 0.60 0.80 0.39 0.68 0.80 0.75	75.12 77.38 74.69 74.00 73.66 73.42 79.55 76.21 70.88 72.18	84.71 84.97 81.14 81.14 81.51 80.41 89.21 83.48 77.50 79.19	0.81 0.77 1.16 0.76 0.86 0.83 0.63 0.94 1.04
CM3 CM4 CM7 CM8 CM10 CM12 CM14 CM16 CM18 CM23 CM24	0.10 0.09 0.10 0.10 0.12 0.08 0.10 0.10 0.10 0.10 0.15	2.96 3.05 5.20 2.62 3.52 2.58 4.86 4.30 3.71 2.87 2.63	4.84 7.26 5.61 6.59 4.55 7.54 3.53 5.89 7.94 7.71 6.36	2.1' 3.09 5.66 2.44 2.56 2.70 2.00 3.88 3.30 2.22	7 9 8 8 0 8 0 6 3 3 6 0 3	0.41 0.66 0.85 0.73 0.60 0.80 0.39 0.68 0.80 0.75 0.66	75.12 77.38 74.69 74.00 73.66 73.42 79.55 76.21 70.88 72.18 72.78	84.71 84.97 81.14 81.14 81.51 80.41 89.21 83.48 77.50 79.19 80.30	0.81 0.77 1.16 0.76 0.86 0.83 0.63 0.94 1.04 0.92
CM3 CM4 CM7 CM8 CM10 CM12 CM14 CM16 CM23 CM24 CM26	0.10 0.09 0.10 0.10 0.12 0.08 0.10 0.10 0.10 0.08 0.15 0.08	2.96 3.05 5.20 2.62 3.52 2.58 4.86 4.30 3.71 2.87 2.63 2.97	4.84 7.26 5.61 6.59 4.55 7.54 3.53 5.89 7.94 7.71 6.36 6.79	2.1' 3.09 5.66 2.44 2.55 2.70 2.00 3.88 3.30 2.22	7 9 8 8 0 6 3 3 6 0 3 3 2	0.41 0.66 0.85 0.73 0.60 0.80 0.39 0.68 0.80 0.75 0.66 0.63	75.12 77.38 74.69 74.00 73.66 73.42 79.55 76.21 70.88 72.18 72.78 72.09	84.71 84.97 81.14 81.14 81.51 80.41 89.21 83.48 77.50 79.19 80.30 79.96	0.81 0.77 1.16 0.76 0.86 0.83 0.63 0.94 1.04 0.92 0.79
CM3 CM4 CM7 CM8 CM10 CM12 CM14 CM16 CM18 CM23 CM24 CM26 CM31	0.10 0.09 0.10 0.12 0.08 0.10 0.10 0.10 0.10 0.08 0.15 0.08 0.09	2.96 3.05 5.20 2.62 3.52 2.58 4.86 4.30 3.71 2.87 2.63 2.97 5.01	4.84 7.26 5.61 6.59 4.55 7.54 3.53 5.89 7.94 7.71 6.36 6.79 4.73	2.1' 3.00 5.6: 2.44 2.5: 2.7' 2.00 3.8: 3.30 2.20 5.5	7 9 8 0 8 0 6 3 6 0 3 3 2 7	0.41 0.66 0.85 0.73 0.60 0.80 0.39 0.68 0.80 0.75 0.66 0.63 1.82	75.12 77.38 74.69 74.00 73.66 73.42 79.55 76.21 70.88 72.18 72.78 72.09 73.06	84.71 84.97 81.14 81.14 81.51 80.41 89.21 83.48 77.50 79.19 80.30 79.96 76.61	0.81 0.77 1.16 0.76 0.86 0.83 0.63 0.94 1.04 0.92 0.79 0.79
CM3 CM4 CM7 CM8 CM10 CM12 CM14 CM16 CM18 CM23 CM24 CM26 CM31 CM33	0.10 0.09 0.10 0.12 0.08 0.10 0.10 0.10 0.10 0.08 0.15 0.08 0.09 0.12	2.96 3.05 5.20 2.62 3.52 2.58 4.86 4.30 3.71 2.87 2.63 2.97 5.01 5.60	4.84 7.26 5.61 6.59 4.55 7.54 3.53 5.89 7.94 7.71 6.36 6.79 4.73 3.96	2.1' 3.00 5.66 2.44 2.55 2.7' 2.00 3.88 3.30 3.00 2.22 2.00 5.55 5.88	7 9 8 0 8 0 6 3 6 0 3 3 2 7 7	0.41 0.66 0.85 0.73 0.60 0.80 0.39 0.68 0.80 0.75 0.66 0.63 1.82 0.23	75.12 77.38 74.69 74.00 73.66 73.42 79.55 76.21 70.88 72.18 72.78 72.09 73.06 85.93	84.71 84.97 81.14 81.14 81.51 80.41 89.21 83.48 77.50 79.19 80.30 79.96 76.61 95.01	0.81 0.77 1.16 0.76 0.86 0.83 0.63 0.94 1.04 0.92 0.79 0.79 0.97
CM3 CM4 CM7 CM8 CM10 CM12 CM14 CM16 CM18 CM23 CM24 CM26 CM31 CM33 CM34	0.10 0.09 0.10 0.10 0.12 0.08 0.10 0.10 0.10 0.08 0.15 0.08 0.09 0.12 0.10	2.96 3.05 5.20 2.62 3.52 2.58 4.86 4.30 3.71 2.87 2.63 2.97 5.01 5.60 4.70	4.84 7.26 5.61 6.59 4.55 7.54 3.53 5.89 7.94 7.71 6.36 6.79 4.73 3.96 4.50	2.1' 3.00 5.6i 2.44 2.5i 2.7' 2.00 3.8i 3.30 2.22 2.0' 5.5' 5.8i 2.7'	7 9 8 8 0 8 0 6 3 3 6 0 3 3 2 7 5 6	0.41 0.66 0.85 0.73 0.60 0.80 0.39 0.68 0.80 0.75 0.66 0.63 1.82 0.23 0.69	75.12 77.38 74.69 74.00 73.66 73.42 79.55 76.21 70.88 72.18 72.78 72.09 73.06 85.93 76.02	84.71 84.97 81.14 81.14 81.51 80.41 89.21 83.48 77.50 79.19 80.30 79.96 76.61 95.01 82.77	0.81 0.77 1.16 0.76 0.86 0.83 0.63 0.94 1.04 0.92 0.79 0.79 0.97 0.97
CM3 CM4 CM7 CM8 CM10 CM12 CM14 CM16 CM18 CM23 CM24 CM26 CM31 CM33 CM34 CM36	0.10 0.09 0.10 0.10 0.12 0.08 0.10 0.10 0.10 0.08 0.15 0.08 0.09 0.12 0.10	2.96 3.05 5.20 2.62 3.52 2.58 4.86 4.30 3.71 2.87 2.63 2.97 5.01 5.60 4.70 3.57	4.84 7.26 5.61 6.59 4.55 7.54 3.53 5.89 7.94 7.71 6.36 6.79 4.73 3.96 4.50 6.75	2.1' 3.0' 5.6' 2.44' 2.5' 2.7' 2.0' 3.8' 3.3' 3.0' 2.2' 2.0' 5.5 5.8' 2.7' 3.0'	7 9 8 8 0 8 0 6 3 3 6 0 3 3 2 7 5 5 6 6 0	0.41 0.66 0.85 0.73 0.60 0.80 0.39 0.68 0.80 0.75 0.66 0.63 1.82 0.23 0.69 0.70	75.12 77.38 74.69 74.00 73.66 73.42 79.55 76.21 70.88 72.18 72.78 72.09 73.06 85.93 76.02 73.45	84.71 84.97 81.14 81.14 81.51 80.41 89.21 83.48 77.50 79.19 80.30 79.96 76.61 95.01 82.77 80.48	0.81 0.77 1.16 0.76 0.86 0.83 0.94 1.04 0.92 0.79 0.79 0.97 0.94 0.74 0.91
CM3 CM4 CM7 CM8 CM10 CM12 CM14 CM16 CM18 CM23 CM24 CM26 CM31 CM33 CM34 CM36 CM39	0.10 0.09 0.10 0.10 0.12 0.08 0.10 0.10 0.10 0.08 0.15 0.08 0.09 0.12 0.10 0.14	2.96 3.05 5.20 2.62 3.52 2.58 4.86 4.30 3.71 2.87 2.63 2.97 5.01 5.60 4.70 3.57 2.13	4.84 7.26 5.61 6.59 4.55 7.54 3.53 5.89 7.94 7.71 6.36 6.79 4.73 3.96 4.50 6.75 7.49	2.1' 3.09 5.66 2.44 2.55 2.70 2.00 3.88 3.30 2.22 2.00 5.5 5.88 2.70 3.00 2.1	7 9 8 8 0 8 8 0 6 3 3 3 6 0 7 5 5 6 6 0 7 7 7 5 6 6 7 7 7 7 7 7 7 7 7 7 7 7 7 7	0.41 0.66 0.85 0.73 0.60 0.80 0.39 0.68 0.80 0.75 0.66 0.63 1.82 0.23 0.69 0.70 0.71	75.12 77.38 74.69 74.00 73.66 73.42 79.55 76.21 70.88 72.18 72.78 72.09 73.06 85.93 76.02 73.45 71.33	84.71 84.97 81.14 81.14 81.51 80.41 89.21 83.48 77.50 79.19 80.30 79.96 76.61 95.01 82.77 80.48 78.85	0.77 1.16 0.76 0.86 0.83 0.63 0.94 1.04 0.92 0.79 0.79 0.97 0.94 0.74 0.91 0.83
CM3 CM4 CM7 CM8 CM10 CM12 CM14 CM16 CM18 CM23	0.10 0.09 0.10 0.10 0.12 0.08 0.10 0.10 0.10 0.08 0.15 0.08 0.09 0.12 0.10	2.96 3.05 5.20 2.62 3.52 2.58 4.86 4.30 3.71 2.87 2.63 2.97 5.01 5.60 4.70 3.57	4.84 7.26 5.61 6.59 4.55 7.54 3.53 5.89 7.94 7.71 6.36 6.79 4.73 3.96 4.50 6.75	2.1' 3.0' 5.6' 2.44' 2.5' 2.7' 2.0' 3.8' 3.3' 3.0' 2.2' 2.0' 5.5 5.8' 2.7' 3.0'	7 9 8 8 0 8 0 6 6 3 3 6 0 7 5 6 6 6 0 7 7 6 6 6 7 7 7 7 7 7 7 7 7 7 7	0.41 0.66 0.85 0.73 0.60 0.80 0.39 0.68 0.80 0.75 0.66 0.63 1.82 0.23 0.69 0.70	75.12 77.38 74.69 74.00 73.66 73.42 79.55 76.21 70.88 72.18 72.78 72.09 73.06 85.93 76.02 73.45	84.71 84.97 81.14 81.14 81.51 80.41 89.21 83.48 77.50 79.19 80.30 79.96 76.61 95.01 82.77 80.48	0.81 0.77 1.16 0.76 0.86 0.83 0.94 1.04 0.92 0.79 0.79 0.97 0.94 0.74 0.91

crust as shown in table 6, the values of the investigated sandstones are within the range of felsic source rock than mafic source rocks. This suggest that the Barail sandstones in Champhai are derived from felsic source rocks. Furthermore, Garver *et al.* (1996) suggest the ultramafic source rock indicated

by elevated concentration of Cr (>150) and Ni (>100) with the ratio of Cr/Ni ranges from 1.3 to 1.5 (Armstrong-Altrin *et al.* 2004, 2013). The Cr (avg. = 122 ppm) and Ni (avg. = 41 ppm) concentration and their ratio (R = 0.58) show the absence of ultramafic source signature in the investigated

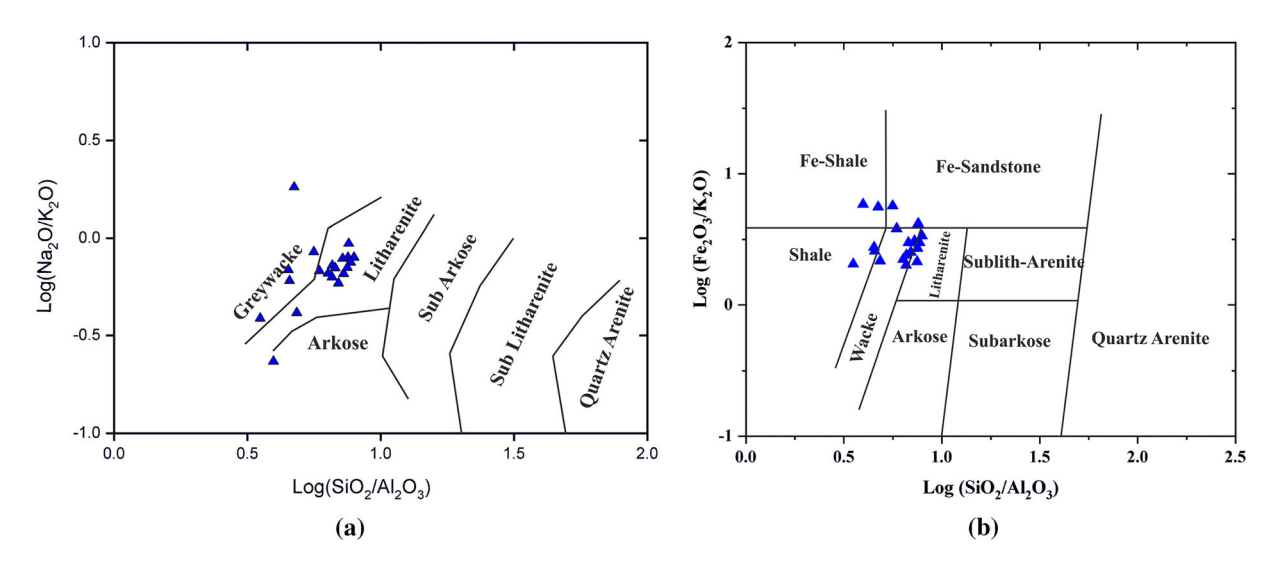


Figure 4. Chemical classification of Barail sandstones in Champhai (a) after Pettijohn et al. (1972) and (b) after Herron (1988).

sandstone. The ratio of Y/Ni and Cr/V are plotted in a binary mixing model curve defined by granite and ultramafic source rock (after Mongelli $et\ al.$ 2006) as shown in figure 7(b). The Cr/V ratio of the studied sandstones is relatively low (avg. = 0.58) and as a result from the plot, the sandstones are clustered more towards the field of granite than the ultramafic field. This suggests the derivation of Barail sandstone from felsic rock with an input of mafic rocks.

A ternary plot of La–Th–Sc (after Jinliang and Xin 2008) shows that the sandstones fall between granite and granodiorite source rock other than basalt. This indicates the derivation of Barail sandstone mainly from felsic and intermediate source (figure 8a).

The immobile trace elements such as V, Ni and Th are used to determine the provenance of clastic sediments by employing ternary plot of V–Ni–Th \times 10 (after Bracciali et al. 2007). Following the plot, the Barail sandstone clustered around and closed towards the felsic source, thus suggesting mixed provenance of felsic source with an input of mafic source (figure 8b).

5.2 Paleoweathering and sediment recycling

The nature of alkali and alkaline earth elements content played an important role in assessing the weathering intensity and duration of sedimentary rocks (Nesbitt and Young 1982). The chemical changes that take place during weathering (i.e., labile elements like Na, Ca and Sr leached and the insoluble elements such as Al, Ba and Rb remains)

imprint in the sedimentary records provide an important information in evaluating the condition of source area weathering (Madharavaju et al. 2016a, b, c; Pandey and Parcha 2017). Different schemes of weathering indices proposed by various workers such as chemical index of alteration (CIA) by Nesbitt and Young (1982), plagical index of alteration (PIA) by Fedo et al. (1995), weathering index of Parker (WIP) by Parker (1970), chemical index of weathering (CIW) by Harnois (1988) and index of chemical variability (ICV) by Cox et al. (1995) are widely used. To decipher the degree of weathering, weathering indices like CIA and PIA are employed and ICV is used to determine compositional maturity. The analysed data of three weathering indices of the investigated sandstone is given in table 3.

The value of CIA is calculated using the following formula:

$$\begin{aligned} \mathrm{CIA} \; &= \; \left[\mathrm{Al_2O_3} / \left(\mathrm{Al_2O_3} + \mathrm{Na_2O} + \mathrm{CaO}^* + \mathrm{K_2O} \right) \right] \\ &\times 100. \end{aligned}$$

where the CaO* represents CaO from the silicate fractions. The CIA value provides the relative proportion of secondary aluminous clay minerals to primary silicate minerals like feldspar. Barail sandstone has a low CaO content in comparison with Na₂O. Therefore, following McLennan (1993) method, the value of CaO is considered as CaO* and is used in the CIA calculation. The CIA value ≤ 50 indicates the near absence of chemical weathering and also reflects cool and arid conditions (Fedo *et al.* 1995). The high value of CIA (76–100)

Table 4. Trace elements composition (ppm) of Barail sandstones in Champhai (where UCC Taylor and McLennan 1985).

Sample	Sc	Λ	Cr	Co	Ni	Cu	Zn	Ga	m Rb	Sr	Y	Z_{Γ}	Nb	$_{ m Ba}$	Pb	Th	U
CM1	08.9	74.00	70.00	10.00	33.00	167.00	183.00	12.00	63.00	61.00	25.00	363.00	12.00	315.00	33.00	16.00	1.31
CM3	12.70	106.00	169.00	9.00	48.00	122.00	192.00	16.00	100.00	81.00	33.00	582.00	18.00	390.00	24.00	22.00	3.39
CM4	7.40	67.00	56.00	12.00	33.00	81.00	188.00	12.00	50.00	39.00	20.00	266.00	9.00	238.00	34.00	15.00	BDL
$_{ m CM7}$	11.30	110.00	141.00	18.00	61.00	193.00	172.00	15.00	72.00	00.99	29.00	256.00	10.00	352.00	29.00	14.00	2.55
CM8	8.20	67.00	63.00	9.00	28.00	157.00	230.00	11.00	59.00	54.00	25.00	428.00	13.00	280.00	36.00	17.00	3.82
CM10	11.70	104.00	108.00	14.00	43.00	111.00	228.00	16.00	94.00	86.00	30.00	281.00	14.00	351.00	19.00	14.00	0.93
CM12	09.9	68.00	49.00	8.00	29.00	00.96	249.00	12.00	55.00	46.00	20.00	235.00	8.00	244.00	17.00	13.00	1.66
CM14	12.20	121.00	208.00	11.00	42.00	97.00	177.00	16.00	00.96	78.00	36.00	522.00	17.00	398.00	19.00	20.00	2.89
CM16	10.50	97.00	153.00	13.00	62.00	67.00	377.00	14.00	68.00	56.00	23.00	327.00	12.00	582.00	23.00	17.00	2.23
CM18	9.90	88.00	124.00	12.00	35.00	47.00	207.00	11.00	62.00	00.09	31.00	595.00	16.00	353.00	16.00	19.00	3.57
CM23	8.70	00.89	185.00	11.00	32.00	105.00	229.00	12.00	64.00	50.00	22.00	251.00	10.00	300.00	16.00	12.00	BDL
CM24	8.30	00.69	00.69	12.00	28.00	90.00	218.00	13.00	70.00	55.00	22.00	290.00	10.00	321.00	18.00	14.00	4.02
CM26	9.00	74.00	94.00	10.00	29.00	70.00	142.00	11.00	68.00	61.00	24.00	367.00	11.00	335.00	12.00	16.00	2.70
CM31	11.90	78.00	147.00	45.00	50.00	64.00	144.00	12.00	41.00	00.69	23.00	175.00	8.00	301.00	16.00	12.00	1.85
CM33	13.40	123.00	242.00	35.00	81.00	121.00	233.00	15.00	65.00	34.00	31.00	508.00	21.00	341.00	21.00	19.00	2.53
CM34	11.80	112.00	169.00	16.00	57.00	92.00	169.00	15.00	73.00	67.00	31.00	435.00	18.00	306.00	15.00	19.00	1.47
CM36	9.90	86.00	61.00	45.00	30.00	95.00	184.00	11.00	57.00	46.00	28.00	410.00	16.00	332.00	13.00	18.00	1.10
CM39	6.40	65.00	52.00	12.00	32.00	71.00	175.00	11.00	64.00	49.00	21.00	239.00	8.00	279.00	16.00	13.00	BDL
CM41	10.50	86.00	198.00	10.00	19.00	57.00	169.00	10.00	39.00	47.00	44.00	######	33.00	336.00	4.00	36.00	6.81
CM45	9.10	88.00	88.00	13.00	40.00	59.00	176.00	13.00	75.00	64.00	27.00	344.00	13.00	381.00	16.00	17.00	1.60
CC	13.60	00.09	83.00	17.00	20.00	25.00	71.00	17.00	112.00	350.00	22.00	190.00	25.00	550.00	20.00	10.70	2.80

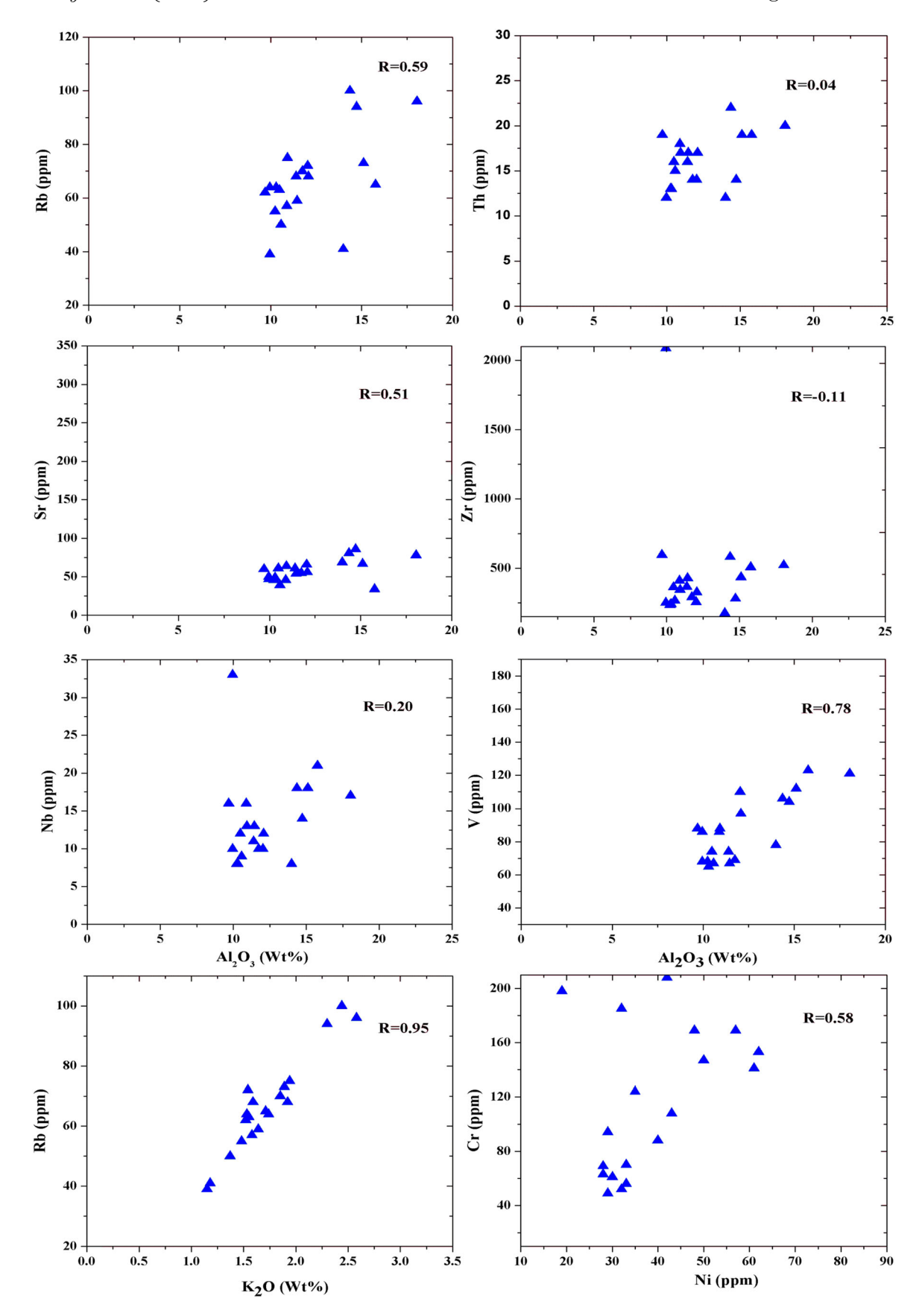


Figure 5. Bivariate diagram showing the correlation of major oxides with trace elements of Barail sandstone.

Table 5. Rare earth elements composition (ppm) of Barail sandstones in Champhai (where UCC Taylor and McLennan 1985).

∑lree/ ∑hree	7.12	10.89	10.77	9.17	10.38	10.52	9.85	10.19	10.22	10.40	9.11	9.16	10.61	10.09	10.35	6.95	9.64	10.91	13.61	10.69	9.54
\sum REE	90.55	226.20	152.03	192.17	193.45	178.62	128.34	227.23	147.16	236.08	128.13	109.26	176.77	245.77	153.29	163.49	210.38	134.84	342.52	206.33	146.37
Lu	0.19	0.31	0.21	0.24	0.24	0.22	0.16	0.31	0.21	0.31	0.19	0.18	0.21	0.33	0.19	0.30	0.24	0.16	0.36	0.22	0.32
$^{\mathrm{Yb}}$	1.45	2.27	1.51	1.92	1.83	1.68	1.25	2.32	1.62	2.36	1.48	1.35	1.69	2.51	1.50	2.40	2.08	1.24	2.60	1.63	2.20
Tm	0.27	0.42	0.27	0.36	0.33	0.31	0.23	0.42	0.29	0.42	0.27	0.24	0.31	0.47	0.28	0.45	0.39	0.23	0.48	0.32	0.33
Er	1.81	2.86	1.91	2.57	2.37	2.23	1.66	2.86	1.95	2.96	1.86	1.66	2.22	3.25	1.97	3.11	2.77	1.61	3.26	2.37	2.30
Но	0.65	86.0	89.0	96.0	0.84	0.80	0.61	1.03	89.0	1.08	0.67	0.59	0.79	1.19	0.70	1.15	1.01	0.57	1.14	0.89	0.80
Dy	3.28	5.25	3.62	5.41	4.70	4.30	3.43	5.57	3.60	5.72	3.61	3.00	4.28	6.29	3.83	6.23	5.66	3.16	6.27	5.11	3.50
Tb	0.59	1.02	0.72	1.12	0.99	0.89	0.69	1.15	0.72	1.17	0.72	0.58	0.86	1.22	0.77	1.17	1.16	0.65	1.31	1.09	0.64
Сd	2.91	5.92	4.00	6.32	5.70	5.07	3.80	6.65	4.05	89.9	3.87	3.15	4.86	6.91	4.27	5.76	6.47	3.70	8.03	6.02	3.80
Eu	98.0	1.63	1.14	1.19	1.47	1.47	1.09	1.81	1.18	1.83	1.12	0.87	1.38	1.86	1.17	1.74	1.80	1.06	1.80	1.72	0.88
$_{ m Sm}$	3.47	7.90	5.56	8.57	7.59	6.81	5.00	8.76	5.49	8.97	5.15	4.08	82.9	9.28	5.81	7.24	8.27	5.14	11.73	8.07	4.50
Nd	15.84	42.00	29.16	39.40	38.95	35.61	24.63	41.75	28.36	43.99	25.10	20.30	35.30	45.74	29.78	32.33	39.46	26.34	62.72	39.06	26.00
\Pr	3.58	10.28	7.01	8.83	9.22	8.36	5.82	10.39	89.9	10.69	5.84	4.84	8.26	10.98	6.91	7.19	9.38	6.21	15.84	9.37	7.10
Ce	40.62	96.77	64.16	78.76	78.86	74.07	53.86	95.81	62.76	00.70	53.20	45.62	72.97	.04.97	65.99	64.55	89.37	56.54	51.98	87.81	64.00
La					40.36																
Sample					CM8 4																

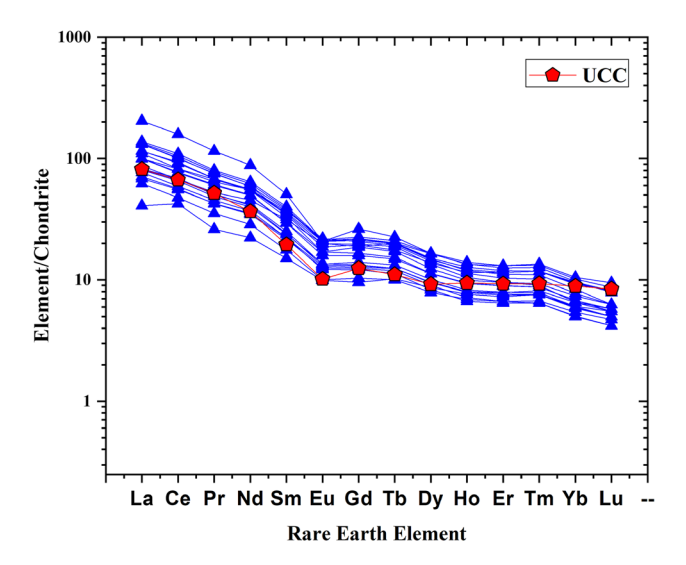


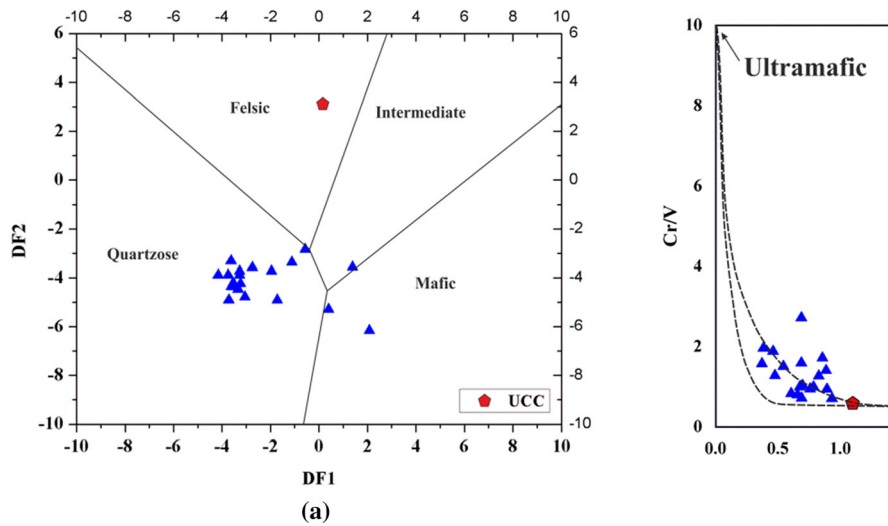
Figure 6. Chondrite normalize REE spider diagram of the investigated sandstones (chondrite values after Taylor and McLennan 1985). The red line indicates Upper Continental Crust (UCC).

represents the intense weathering in the source area (Nesbitt and Young 1982; Madhavaraju et al. 2016a, b, c; Pandey and Parcha 2017). The CIA values of Barail sandstones in Champhai range between 70.88 and 85.93 with an average of 74.52. The CIA values indicated that the Barail sandstone are derived from moderate to intense weathering and thus suggested that the provenance might be subjected to high chemical breakdown.

Furthermore, the chemical weathering of sediments can be evaluated by Plagioclase Index of Alteration (PIA). The formula of PIA calculation is given below:

$$PIA = [(Al_2O_3 - K_2O)/(Al_2O_3 + Na_2O + CaO^* - K_2O)] \times 100 \text{ (molecular proportion)}.$$

The maximum value of PIA is 100 for complete altered materials (kaolinite and gibbsite) and



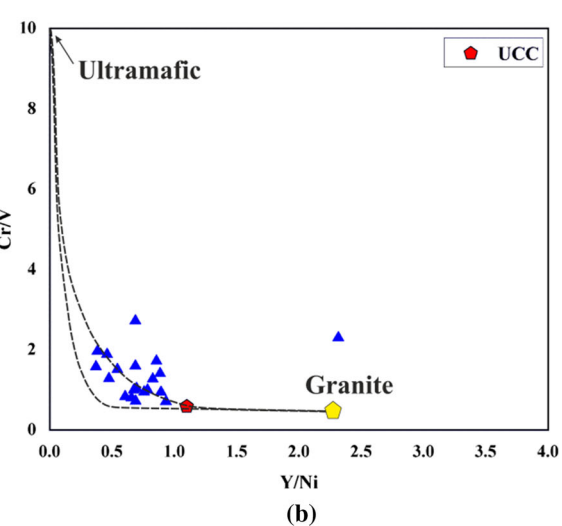


Figure 7. (a) Major element discriminant function diagram of Barail sandstones in Champhai after Roser and Korsch (1988). (b) Binary plot of Y/Ni and Cr/V for granite-ultramafic end member mixing (after Mongelli *et al.* 2006).

Table 6. Comparisons of the elemental ratio of Barail sandstones in Champhai with elemental ratio of other source rocks.

Elemental ratio	Rang of Barail sandstone	Felsic sources ¹	Mafic sources ¹	UCC $(T\&M)^2$
Eu/Eu*	0.54 - 0.81	0.40 – 0.83	0.71 – 0.95	0.63
La/Lu	8.21-21.63	3.00 – 27.0	1.10 - 7.00	9.73
La/Sc	2.21 - 7.14	2.50 – 16.3	0.43 – 0.86	2.21
La/Co	0.86 - 7.50	1.80 - 13.8	0.14 – 0.38	1.76
Th/Sc	1.01 - 3.43	0.84 – 20.5	0.05 – 0.22	0.79
Th/Co	0.27 – 3.60	0.67 - 19.4	0.04 - 1.40	0.63
Cr/Th	3.39 - 15.42	4.00 – 15.00	25 - 500	7.76

¹Cullers et al. (1988), Cullers (1994, 2000), Cullers and Podkovyrov (2000).

²Taylor and McLennan (1985).

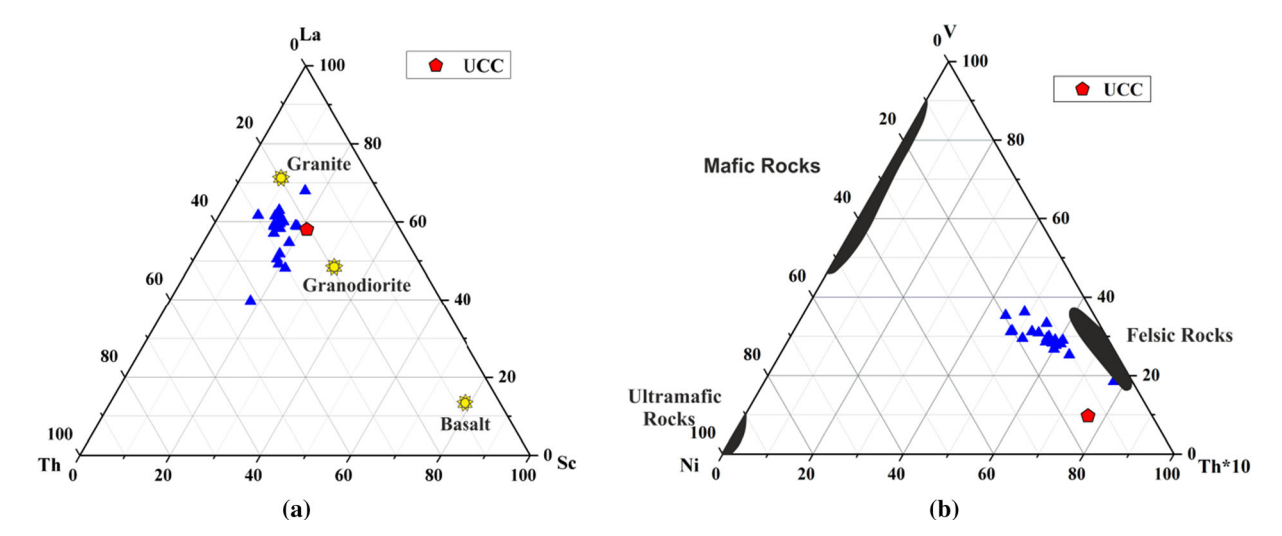


Figure 8. (a) La–Th–Sc ternary plot of Barail sandstone (after Jinliang and Jin 2008). (b) Ternary plot of V–Ni–Th×10 (after Bracciali et al. 2007).

weathered plagioclase has a PIA value of 50. The PIA values of the studied sandstone samples range from 76.61 to 95.01 with an average of 81.82 which are consistent with CIA value showing moderate to intense chemical weathering in the source rock.

Geochemical data of Champhai sandstone were plotted in an A-CN-K diagram (figure 9a) proposed by Nesbitt and Young (1982). From this diagram, the original source rock composition, mobility of elements during the process of chemical weathering of source material and post-depositional chemical modification can be determined. In the A-CN-K diagram, the sandstones fall parallel to A-CN above the feldspar join. This is due to the leaching out of Na₂O and CaO from earlier dissolve plagioclase. This indicates the initial stage of weathering (Fedo et al. 1995). The plot run closer to illite on the A–K line and trend slightly towards Al₂O₃ but showing no inclination towards the K apex. This indicated that the sandstones are free from potash metasomatism during diagenesis. However, the A-CN-K diagram shows the weathering trend as moderate to intense weathering conditions.

During chemical weathering, oxidations of $\rm U^{4+}$ to $\rm U^{6+}$ occur that leads to the elevation in Th/U ratio. Th/U ratio of upper crustal rock has a range of 3.5–4.0 (McLennan *et al.* 1993; Bhuiyan *et al.* 2011; Madhavaraju *et al.* 2016a, b, c) where the ratio > 4.0 indicates high intense weathering or sediment recycling in a source area. The Th/U ratio ranges from 3.48 to 16.36 with an average of

7.98. This suggests derivation of the rocks from recycled sediments with intensive weathering in the source area.

In addition, the ratio of Zr/Sc and Th/Sc provides an important signature of provenance and sediment recycling of a source area. From the plotting of Zr/Sc vs. Th/Sc (after McLennan et al. 1993), the studied sediments follow the compositional trend that designated volcanic rocks such as basalt, andesite, dacite, granodiorite and rhyolite (after Roser and Korsch 1999). Most of the samples are clustered around rhyolite composition with few samples falls near granodiorite field. Besides, the high ratio of Zr/Sc indicates the enrichment of zircon thus suggest sediment recycling (figure 9b).

The sediment maturity can be determined by calculating the index compositional variation (ICV) using the following formula proposed by Cox et al. (1995):

$$ICV = (Fe2O3 + K2O + Na2O + CaO + MgO + MnO + TiO2)/Al2O3.$$

The ICV value of the investigated sandstones ranges between 0.63 and 1.16 (only two samples show ICV value higher than 1). The average value of ICV (0.88) shows that the studied sandstones are compositionally mature and deposited in the tectonically quiescent or cratonic environment (Pandey and Parcha 2017). Furthermore, plotting of CIA vs. ICV (after Long et al. 2012) shows that the sediments are

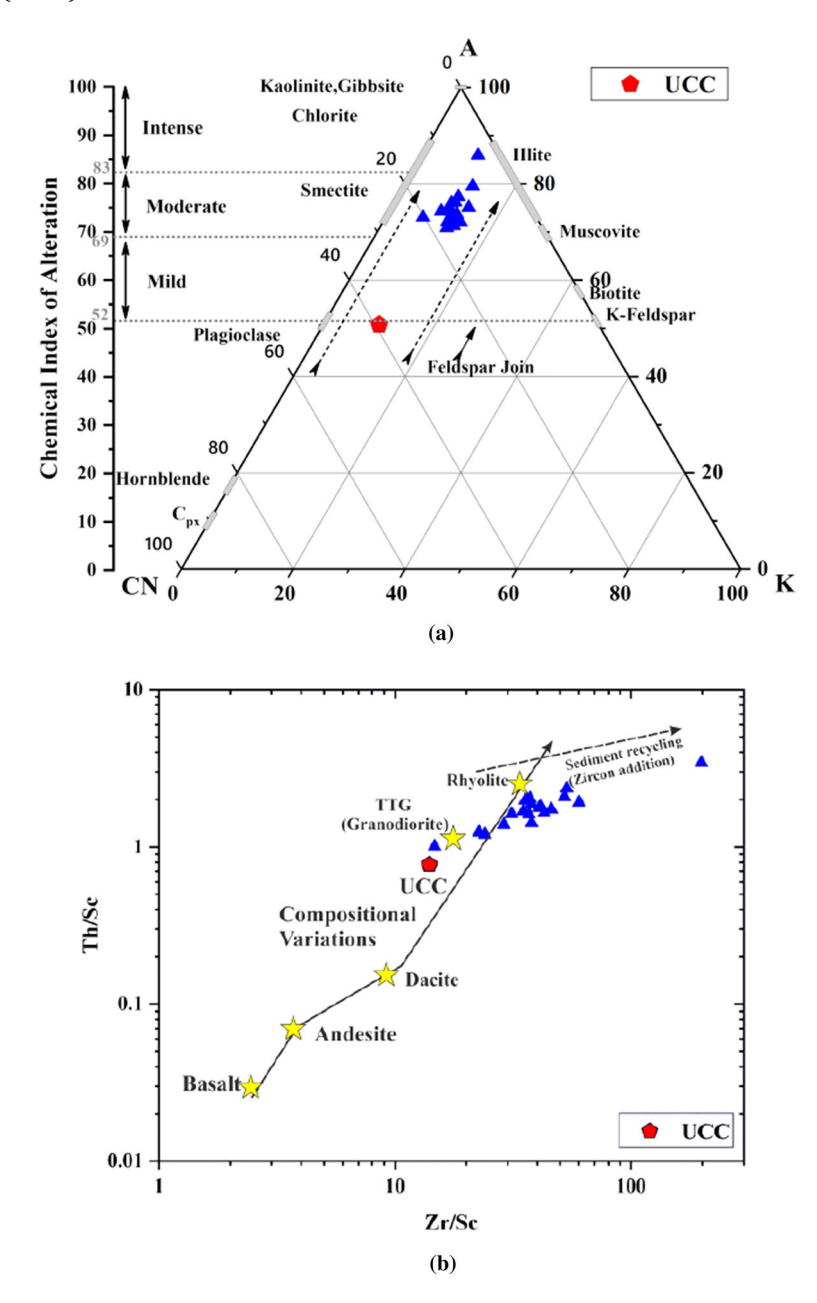


Figure 9. (a) A–CN–K ternary diagram showing the weathering trend of Barail sandstones in Champhai, compared with UCC (Rudnick and Gao 2003). (b) Plotting of Zr/Sc vs. Th/Sc (McLennan et al. 1993) where stars: basalt, andesite and rhyolite are average volcanic rock compositions (as plotted by Roser and Korsch 1999).

chemically mature with intense weathering in the source rock (figure 10). The sediment maturity can also be determined with the help of $\mathrm{SiO}_2/\mathrm{Al_2O_3}$ ratio, the ratio >5 indicate mature sandstone while the ratio <5 is an indication of immaturity (Roser and Korsch 1988; Roser et al. 1996). The value of $\mathrm{SiO}_2/\mathrm{Al_2O_3}$ in the studied sandstone ranges from 3.53 to 7.94 (average = 6.18) which indicate immature character to progressive maturity of Barail sandstone (Roser et al. 1996), and the values of $\mathrm{K}_2\mathrm{O}/\mathrm{Na}_2\mathrm{O}_3$

ratio range from 0.55 to 4.28 (average = 1.61). The high values of SiO_2/Al_2O_3 ratio indicated maturity of Barail sandstones in terms of mineralogical maturity. As per ICV values, the studied rocks are showing close affinity to mature mudstones which are depleted in silicate than clay, so in classification they also fall under wacke and litharenite which are immature; in addition, the SiO_2/Al_2O_3 ratios of the rocks also partly indicated mineralogical immaturity to progressive maturity of the rock.

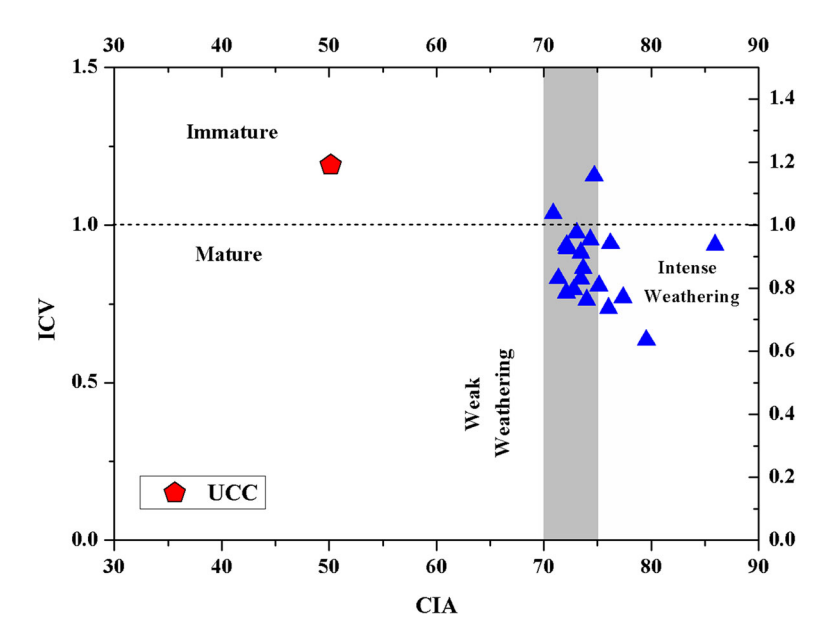


Figure 10. CIA vs. ICV binary plot (after Long et al. 2012) of Barail sandstone.

6. Conclusion

- The investigated Barail sandstones are classified as litharenite, sublitharenite and wacke which are found to be derived from quartzose recycled orogen.
- 2. The positive correlation of Rb with K₂O implies that the elements are controlled by clay minerals and concentrated during weathering.
- 3. The discriminant function diagram after Roser and Korsch (1988) shows that the investigated sandstones are derived from recycled continental provenance. The chondrite normalised REE represented enrichment of LREE and depletion of HREE, where a high LREE/HREE ratios and negative Eu anomaly suggest derivation of the investigated sandstone from felsic igneous source. The ratio of elements such as (La/Lu)_{cn}, Eu/Eu, La/Sc, La/Co, Cr/Th, Th/Sc, and Th/Co also revealed the provenance to be of felsic source rock.
- 4. The elevated Cr and Ni concentration and their low ratio represent the absence of ultramafic source signature, while the binary plot of Y/Ni and Cr/V suggested that the derivation of Barail sandstone from felsic rock with an input of mafic rocks.
- 5. The clustered nature of Barail sandstone in the field of granite and granodiorite in ternary plot of La–Th–Sc indicated derivation of the Barail sandstone from felsic and intermediate source.

- 6. The A-CN-K diagram indicated moderate to intense weathering conditions. The Zr/Sc vs. Th/Sc diagram has shown the affinity of the sandstones to granodiorite and rhyolite which further suggested the sediment recycling with an addition of zircon.
- 7. The CIA and PIA revealed the paleoweathering condition of Barail sediments as moderate to intense weathering in the source area. Furthermore, the ICV value, the plot of CIA vs. ICV and the ratio of SiO₂/Al₂O₃ indicated mineralogical immaturity to progressive maturity of the rock.
- 8. Sediments of the investigated Barail sandstone are found to be derived from wide spectrum of protoliths ranging from recycled sedimentary terrain to intermediate to mafic/felsic sources of Himalaya. The history of weathering in the provenance was also varied with the variation in lithology which had undergone moderate to intense weathering.

Acknowledgements

The authors are deeply thankful DST-SERB for funding the research in the form of project. The authors would like to acknowledge the Director, National Geophysical Research Institute (NGRI), Hyderabad and Wadia Institute of Himalayan Geology (WIHG), Dehradun for their kind permission to do geochemical analysis. The authors

also thank the authority of Mizoram University for support to do the project work. Funding was provided by Science and Engineering Research Board (Grant No. EEQ/2016/000655).

Author statement

The authors Jimmy Lalnunmawia, Malsawmtluangkima Hauhnar and Orizen M S Dawngliana contribute equally in various analytical works, plotting of all figures using software and other computer applications and the interpretations of data. Each author read and approved the final manuscript.

References

- Al-Juboury A 2007 Petrography and major element geochemistry of Late Triassic Carpathian keuper sandstones: Implications for provenance; Bulletine de l'Institute Scientifique, Rabat, section science de la Terre 29 1–14.
- Armstrong-Altrin J S, Lee Y and Ramasamy S 2004 Geochemistry of sandstones from the Upper Miocene Kudankulam Formation, Southern India: Implications for provenance, weathering and tectonic setting; *J. Sed. Res.* **74** 285–297.
- Armstrong-Altrin J S, Nagarajan R, Madhavaraju J, Rosalez-Hoz L, Lee Y I, Balaram V, Cruz-Martinez A and Avila-Ramirez G 2013 Geochemistry of the Jurassic and Upper Cretaceous shales from the Molango Region, Hidalgo, Eastern Mexico: Implications of source-area weathering, provenance, and tectonic setting; C. R. Geosci. 345 185–202.
- Behra U K, Mohanty, B K, Lahiri S, Ray J N, Gupta G D, Prakash H S M and Kesari G K 2011 Geology and mineral resources of Manipur, Mizoram, Nagaland and Tripura; Geol. Surv. India Misc. Pub. No. 30(4) 1(2) 103.
- Bharali B, Borgohain P, Bezbaruah D, Vanthangliana V, Phukan P P and Rakshit R 2017 A geological study on Upper Bhuban Formation in parts of Surma Basin, Aizawl, Mizoram; Sci. Vis. 17(3) 128–147.
- Bhatia M R 1983 Plate tectonics and geochemical composition of sandstones; *J. Geol.* **91** 611–627.
- Bhuiyan M A H, Rahman M J J, Dampare S B and Suzuki S 2011 Provenance, tectonics and source weathering of modern fluvial sediments of the Brahmaputra–Jamuna River, Bangladesh: Inference from geochemistry; *J. Geochem. Expl.* 111 113–137.
- Bracciali L, Marroni M, Pandolfi L and Rocchi S 2007 Geochemistry and petrography of Western Tethys Cretaceous sedimentary covers (Corsica and Northern Apennines): From source areas to configuration of margins; In: Sedimentary provenance and petrogenesis: Perspectives from petrography and geochemistry (eds) Arribas J, Critelli S and Johnsson M J; Geol. Soc. Am. Spec. Paper 420 73–93.
- Chaudhuri A, Baneerjee S and Chauhan G 2020 Compositional evolution of silica clastic sediments recording the

- tectonic stability of a pericratonic rift: Mesozoic Kutch Basin, western India; Mar. Petrol. Geol. 111 476–495.
- Cox R, Lower D R and Cullers R L 1995 The influence of sediment recycling and basement composition on evolution of mudrock chemistry in the southwestern United States; *Geochim. Cosmochim. Acta* **59** 2919–2940.
- Cullers R L 1994 The controls on the major and trace element variation of shales, siltstones and sandstones of Pennsylvanian–Permian age from uplifted continental blocks in Colorado to platform sediment in Kansas, USA; Geochim. Cosmochim. Acta 58 4955–4972.
- Cullers R L 1995 The controls on the major and trace element evolution of shales, siltstones and sandstones of Ordovician to Tertiary age in the Wet Mountain region, Colorado, USA; Chem. Geol. 123 107–131.
- Cullers R L 2000 The geochemistry of shales, siltstones and sandstones of Pennsylvanian–Permian age, Colorado, USA: Implications for provenance and metamorphic studies; Lithos 51 181–203.
- Cullers R L and Podkovyrov V N 2000 Geochemistry of the Mesoproterozoic Lakhanda shales in southeastern Yakutia, Russia: Implications for mineralogical and provenance control, and recycling; *Precamb. Res.* 104 77–93.
- Cullers R L, Basu A and Suttner L J 1988 Geochemical signature of provenance in sand-size material in soils and stream sediments near the Tobacco Root Batholith, Montana, USA; Chem. Geol. 70 335–348.
- Dickinson W R, Beard L S, Brakenridge G R, Erjavec J L, Ferguson R C, Inman K F, Knepp R A, Lindberg F A and Ryberg P T 1983 Provenance of North American Phanerozoic sandstones in relation to tectonic setting; Geol. Soc. Am. Bull. 94 222–235.
- Evans P 1964 Tectonic framework of Assam; J. Geol. Soc. India 48 17–26.
- Fedo C M, Nesbitt H W and Young G M 1995 Unravelling the effects of potassium metasomatism in sedimentary rocks and paleosols, with implications for paleoweathering condition and provenance: *Geology* 23 921–924.
- Folk R L 1974 Petrology of sedimentary rocks; Hemphill, Austin. Ganguly S 1975 Tectonic evolution of the Mizo Hills; Bull. Geol. Min. Met. Soc. India 48 28–40.
- Ganju J L 1975 Geology of Mizoram; Bull. Geol. Min. Met. Soc. India 48 17–26.
- Garver J I, Royce P R and Smick T A 1996 Chromium and nickel shale of the Taconic Foreland: A case study for the provenance of fine-grained sediments with an ultramafic source; J. Sedim. Res. 66 100–106.
- Harnois L 1988 The CIW index: A new chemical index of weathering; Sedim. Geol. 55 319–322.
- Hauhnar M and Lalnunmawia J 2018 Petrography of Barail sandstone of Champhai–Mualkawi section in Champhai district, Mizoram: Implication on provenance and tectonic setting; Adv. Eng. Res. 178 66–73.
- Hayashi K I, Fujisawa H, Holland H D and Ohmoto H 1997 Geochemistry of 1.9 Ga sedimentary rocks from northeastern Labrador, Canada; Geochim. Cosmochim. Acta 61 4115–4137.
- Herron M M 1988 Geochemical classification of terrigenous sands and shales from core or log data; *J. Sedim. Res.* **58** 820–829.
- Hofer G, Wagreich M and Neuhuber S 2012 Geochemistry of fine-grained sediments of the Upper Cretaceous to

- Paleogene Gosau Group (Austria, Slovakia): Implication for paleoenvironmental and provenance studies; *Geosci. Frontiers* 4 449–468.
- Hussain M F and Bharali B 2019 Whole-rock geochemistry of Tertiary sediments of Mizoram Foreland Basin, NE India: Implications for source composition, tectonic setting and sedimentary processes; Acta Geochim. 38 897–914.
- Ingersoll R V, Bullard T F, Ford R L, Grimm J P, Pickle J D and Sares S W 1984 The effect of grain size on detrital modes: A test of the Gazzi–Dickinson pointcounting method; J. Sedim. Petrol. 54 103–116.
- Jinliang Z and Xin Z 2008 Composition and provenance of sandstones and siltstones in Paleogene, Huimin depression, Bohai Bay basin, eastern China; J. China Univ. Geosci. 19 252–270.
- Karunakaran C 1974 Geology and mineral resources of the states of India; *Misc. Publ. Geol. Surv. India* **30(4)** 93–101.
- Kichu A M and Srivastava S K 2018 Diagenetic environment of Barail Sandstones in and around Jotsoma Village, Kohima District, Nagaland, India; J. Geosci. Res. 3(1) 31–35.
- La Touche 1891 Note on the geology of Lushai Hills; Rec. Geol. Surv. India 24 83–141.
- Lalduhawma K and Kumar S 2014 Petrochemistry of Bhuban Formation rocks in and around Aizawl City, Mizoram, India; Sci. Vis. 14(2) 71–83.
- Lalmuankimi C, Kumar S and Tiwari R P 2011 Geochemical study of upper Bhuban sandstone in Muthi, Mizoram, India; Sci. Vis. 11(1) 40–46.
- Lalnunmawia J and Lalhlimpuii J 2014 Classification and provenance studies of the sandstones exposed along Durtlang road section, Aizawl, Mizoram; Sci. Vis. 14(3) 158–167.
- Lalnunmawia J, Vabeihmo Ch and Lalremruatsanga H 2016 Petrography and heavy minerals as tools for reconstruction of provenance and depositional environment of Bhuban sandstones in Aizawl, Mizoram; Sci. Vis. 16 1–9.
- Long X, Yan C, Sun M, Wang Y, Cai K, Jiang Y 2012 Geochemistry and Nd isotopic composition of the Early Paleozoic flysch sequence in the Chinese Itai, central Asia: Evidence for a northward-derived mafic source and insight into Nd model ages in accretionary orogen; *Gondwana Res.* 22 554–566.
- Madhavaraju J 2015 Geochemistry of Campanian–Maastrichtian sedimentary rocks in the Cauvery basin, south India; In: Constraints on paleoweathering, provenance and Cretaceous environments (ed.) Ramkumar M, Chemostratigraphy: Concepts, Techniques and Applications, Elsevier Spec. Vol., pp. 185–214.
- Madhavaraju J, Loser H, Lee Y I, Lozano-Santacruz R and Pi-Puig T 2016a Geochemistry of Lower Cretaceous Limestones of the Alisitos Formation, Baja California, Mexico: Implications for REE source and paleo-redox conditions; *J. South Am. Earth Sci.* **66** 149–165.
- Madhavaraju J, Ramirez-Montoya E E, Monreal R, Gonzalez-Leon C M, Pi-Puig T, Espinoza-Maldonado I G and Grijalva-Noriega F J 2016b Paleoclimate, paleoweathering and paleoredox conditions of Lower Cretaceous shales from the Mural Limestone, Tuape section, northern Sonora, Mexico: Constraints from clay mineralogy and geochemistry; Revista Mexicana De Ciencias Geologicas 33(1) 34–48.

- Madhavaraju J, Tom M, Lee Y I L, Balaram V, Ramasamy S, Carranza-Edwards A and Ramachandran A 2016c Provenance and tectonic settings of sands from Puerto Penasco, Desemboque and Bahia Kino beaches, gulf of California, Sonora, Mexico; J. South Am. Earth Sci. 71 262–275.
- Madhavaraju J, Pacheco-Olivas S A, Gonzalez-León C M, Espinoza-Maldonado I G, Sanchéz-Medrano P A, Villanueva-Amadoz U, Monreal R, Pi-Puig T, Ramírez-Montoya E and Grijalva-Noriega F J 2017 Mineralogy and geochemistry of the Lower Cretaceous siliciclastic rocks of the Morita Formation, Sierra San José section, Sonora, Mexico; J. South Am. Earth Sci. 76 397–411.
- Madhavaraju J, Saucedo-Samaniego J C, Löser L, Espinoza-Maldonado I G, Solari L, Monreal R, Grijalva-Noriega F J and Jaques-Ayala C 2019 Detrital zircon record of Mesozoic volcanic arcs in the Lower Cretaceous Mural Limestone, northwestern Mexico; Geol. J. 54 2621–2645.
- McLennan S M, Hemming S, McDaniel D K and Hanson G N 1993 Geochemical approaches to sedimentation, provenance and tectonics; *Geol. Soc. Am. Spec. Paper* **284** 295–303.
- Mongelli G, Critelli S, Perri F, Sonnino M and Perrone V 2006 Sedimentary recycling, provenance and paleoweathering from chemistry and mineralogy of Mesozoic continental red bed mudrocks, Peloritani Mountains, Southern Italy; Geochem. J. 40 197–209.
- Nandy D R 2017 Geodynamics of northeastern India and the adjoining Region; Scientific Book Centre, Guwahati, Assam, 272p.
- Nesbitt H W and Young G M 1982 Early Proterozoic climates and plate motions inferred from major elements of lutites; Nature 299 715–717.
- Oni S O, Olatunj A S and Ehinola O A 2014 Determination of provenance and tectonic settings of Niger Delta clastic facies using Well-Y, Onshore Delta States, Nigeria; *J. Geochem.*, https://doi.org/10.1155/2014/960139.
- Pandey S and Parcha S K 2017 Provenance, tectonic setting and source-area weathering of the lower Cambrian sediments of the Parahio valley in the Spiti basin, India; *J. Earth Syst. Sci.* **126** 27.
- Parker A 1970 An index of weathering for silicate rocks; Geol. Mag. 107 501–504.
- Pettijohn F J, Potter P E and Siever R 1972 Sand and Sandstone; Springer-Verlag, 241p.
- Rahman J J M and Suzuki S 2007 Geochemistry of sandstones from the Miocene Surma Group, Bengal Basin, Bangladesh: Implications for Provenance, tectonic setting and weathering; *Geochem. J.* 41 415–428.
- Ramachandran A, Madhavaraju J, Ramasamy S, Lee Y I L, Rao S, Chawngthu D L and Velmurugan K 2015 Geochemistry of Proterozoic clastic rocks of the Kerur Formation of Kaladgi–Badami Basin, North Karnataka, South India: Implications for paleoweathering and provenance; *Turkish J. Earth Sci.* 25.
- Ramamoorthy A and Ramasamy S 2015 Petrography and Provenance of Surface Barail Sandstones, Kohima, Nagaland, India; *Int. J. Engr. Mgmt. Eco.* **4(10)** 35–41.
- Roser B P and Korsch R J 1988 Provenance signatures of sandstone–mudstone suites determined using discrimination function analysis of major element data; *Chem. Geol.* **67** 119–139.

- Roser B P and Korsch R J 1999 Geocehmical characterization, evolution and source of Mesozoic accretionary wedge: The Torlesse terrane, New Zealand; *Geol. Maq.* **136** 493–512.
- Roser B P, Cooper R A, Nathan S and Tulloch A J 1996 Reconnaissance sandstone geochemistry, provenance, and tectonic setting of the lower Paleozoic terranes of the West Coast and Nelson, New Zealand; J. Geol. Geophys. 39 1–16.
- Sen S, Das P K, Bhagaboty B and Singha L J C 2012 Geochemistry of shales of Barail group occuring in and around Mandardisa, North Cachar Hills, Assam, India: Its Implications; *Int. J. Chem. Appl.* 4(1) 25–37.

Corresponding editor: Santanu Banerjee

- Srivastava S K and Pandey N 2011 Search for Provenance of Oligocene Barail sandstones in and around Jotsoma, Kohima, Nagaland; *J. Geol. Soc. India* **77** 433–442.
- Taylor S R and McLennan S M 1985 The continental crust: Its composition and evaluation; Oxford: Blackwell, 312p.
- Tiwari R P and Kachhara R P 2003 Molluscan biostratigraphy of the tertiary sediments of Mizoram, India; *J. Paleon. Soc. India* 48 59–82.
- Zoramthara C, Ralte V Z and Lalramdina P 2015 Grain size analysis of Tipam sandstones near Buhchang village, Kolasib district, Mizoram; Sci. Vis. 15 42–51.